JOURNAL OF GEOPHYSICAL RESEARCH, VOL. 103, NO. D3, PAGES 3571–3585, FEBRUARY 20, 1998

Measurements of reactive nitrogen in the stratosphere

B. Sen, G. C. Toon, G. B. Osterman, J.-F. Blavier, J. J. Margitan, and R. J. Salawitch

Jet Propulsion Laboratory, California Institute of Technology, Pasadena

G. K. Yue

NASA Langley Research Center, Hampton, Virginia

Abstract. We present volume mixing ratio profiles of NO, NO_2, HNO_3, HNO_4, N_2O_5, and $ClNO_3$ and their composite budget (NO_y), from 20 to 39 km, measured remotely in solar occultation by the Jet Propulsion Laboratory MkIV Interferometer during a balloon flight from Fort Sumner, New Mexico (35°N), on September 25, 1993. In general, observed profiles agree well with values calculated using a photochemical steady state model constrained by simultaneous MkIV observations of long-lived precursors and aerosol surface area from the Stratospheric Aerosol and Gas Experiment II. The measured variation of concentrations of NO_x (= NO + NO_2) and N_2O_5 between sunrise and sunset reveals the expected ~2:1 stoichiometry at all altitudes. Despite relatively good agreement between theory and observation for profiles of NO and HNO_3 the observed concentration of NO_2 becomes progressively higher than model values below 30 km, with the discrepancy reaching ~30% at 22 km. This suggests an incomplete understanding of factors that regulate the NO/NO_2 and NO_2/HNO_3 ratios below 30 km. Observations obtained during September 1990, prior to the June 1991 eruption of Mount Pinatubo, as well as during April 1993 and September 1993 provide a test of our understanding of the affect of aerosol surface area on the NO_x/NO_y ratio at midlatitudes. The observations reveal a decrease in the NO_x/NO_y ratio for increasing aerosol surface area that is consistent with the heterogeneous hydrolysis of N_2O_5 being the dominant sink of NO_x between altitudes of 18 and 24 km for the conditions encountered (e.g., surface areas as high as 14 μm^2 cm^{-3} and temperatures from 209 to 219 K).

1. Introduction

Reactions involving NO and NO_2 [e.g., *Crutzen*, 1970; *Johnston*, 1971] constitute the primary process for chemical removal of stratospheric O_3 between altitudes of ~24–36 km [*Jucks et al.*, 1996; *Osterman et al.*, 1997]. The abundance of NO_x (= NO + NO_2) regulates the concentration of chlorine monoxide (ClO) as well as the ratio of OH to HO_2 in the midlatitude lower stratosphere for air unaffected by polar stratospheric clouds [e.g., *Wennberg et al.*, 1994]. The partitioning of NO_y between N_2O_5 and HNO_3, the dominant reservoirs of the nitrogen oxide family of gases (NO_y, defined as the sum of the concentration of NO_x, HNO_3, HNO_4, $2{\cdot}N_2O_5$, $ClNO_3$, $BrNO_3$, NO_3, and HNO_2), is controlled by a variety of processes, including some occurring on the surface of sulfate aerosols [e.g., *McElroy et al.*, 1992].

Increased aerosol loading following the eruption of Mount Pinatubo in June 1991 led to reduced levels of NO_x, increased concentrations of ClO, and accelerated photochemical removal of O_3 near 20 km, consistent with the heterogeneous reaction of N_2O_5 + H_2O being the dominant sink for NO_x [e.g., *Fahey et al.*, 1993; *Kawa et al.*, 1993; *Salawitch et al.*, 1994a, b; *Stimpfle et al.*, 1994]. Balloon-borne in situ observations of NO, NO_y, O_3, and aerosol surface area [*Kondo et al.*, 1997]; NO_2 and HNO_3 [*Webster et al.*, 1994]; and ClO, NO, and O_3 [*Dessler et al.*, 1993] each show a reduction in NO/NO_y for increased aerosol loading consistent with chemistry driven largely by the heterogeneous hydrolysis of N_2O_5. Similar conclusions were reached by *Morris et al.* [1997] on the basis of analysis of sunset measurements of NO and NO_2 by the Halogen Occultation Experiment (HALOE), correlated nighttime measurements of HNO_3 and $ClNO_3$ by the Cryogenic Limb Array Etalon Spectrometer (CLAES), and measurements of aerosol by the Stratospheric Aerosol and Gas Experiment II (SAGE II). However, ground-based observations of the decrease in the column abundance of NO_2 and simultaneous increase in column HNO_3 following the eruption of Mount Pinatubo indicate the need for additional heterogeneous sinks of NO_x to quantitatively account for the measured decrease in NO_2/HNO_3 [*Koike et al.*, 1994]. In situ observations of NO, NO_2, ClO, and O_3 at midlatitudes during the spring of 1993 have revealed a troubling discrepancy in our understanding of the NO/NO_2 ratio near 20 km [*Jaeglé et al.*, 1994], although more recent observations over a wider range of latitudes reveal good agreement between theory and observation of this ratio as well as the NO_x/NO_y ratio [*Gao et al.*, 1997]. Finally, an analysis of in situ observations of HCl obtained from 1991 to 1996 suggests heterogeneous reactions other than N_2O_5 + H_2O exert a dominant influence on the composition of the midlatitude stratosphere (C. R. Webster et al., Evolution of HCl concentrations in the lower stratosphere from 1991 to 1996 following the eruption of Mount Pinatubo, submitted to *Geophysical Research Letters*, 1997, hereinafter referred to as Webster et al., submitted manuscript, 1997).

Paper number 97JD02468.
0148-0227/98/97JD-02468$09.00

The Jet Propulsion Laboratory (JPL) Mark IV Interferometer (MkIV) balloon observations reported here represent the first simultaneous measurements of profiles for all major NO_y species in the same air mass along with the important precursors (e.g., O_3, CH_4, H_2O, C_2H_6, HCl, and CO) that allow for a stringent comparison to calculated profiles. Furthermore, noon, sunset, and sunrise profiles of NO_x and N_2O_5 were measured, allowing their diurnal behavior to be examined. Previous studies of the diurnal behavior of these gases have either obtained measurements over a limited altitude range [*Webster et al.*, 1990; *Kondo et al.*, 1990], have not measured all the relevant species [*Roscoe et al.*, 1981; *Chance et al.*, 1996], or have not measured them all simultaneously in the same air mass [*Russell et al.*, 1988; *Rinsland et al.*, 1996].

Our analyses of the MkIV observations test our understanding of processes that regulate (1) NO_x, the component of NO_y that reacts directly with O_3, (2) HNO_3, the dominant NO_y species at low altitudes, (3) N_2O_5, the component that links reactive and reservoir NO_y, (4) HNO_4, a minor reservoir that tests our understanding of HO_x (= OH + HO_2), and (5) $ClNO_3$, the species that couples reactive nitrogen and chlorine. Additionally, our study focuses on testing our understanding of the processes that regulate the concentration of NO_x between 20 and 40 km altitude for various levels of aerosol loading prior to and following the eruption of Mount Pinatubo. Profiles of aerosol surface area associated with each MkIV flight originate from SAGE II analyses of zonal, monthly mean measurements of extinction [*Yue et al.*, 1994].

2. Balloon Measurements

The MkIV Interferometer [*Toon*, 1991] is the latest solar absorption Fourier transform infrared (FTIR) spectrometer designed at JPL for the purpose of remotely measuring atmospheric composition. The brightness and stability of the Sun allow high signal-to-noise ratio spectra with broad coverage (650–5650 cm^{-1}) to be obtained at high spectral resolution (0.01 cm^{-1}), allowing the abundances of a large number of gases to be measured simultaneously, including NO, NO_2, HNO_3, HNO_4, N_2O_5, $ClNO_3$, O_3, N_2O, H_2O, CH_4, HCl, HOCl, CO, and C_2H_6. Very long absorption paths through the atmosphere are obtained by viewing the rising or setting Sun, yielding high sensitivity to these trace species. From a series of such spectra measured at different tangent altitudes the volume mixing ratio (vmr) profiles of these gases may be retrieved.

The solar infrared spectra analyzed in this work were acquired during three balloon flights, from Fort Sumner, New Mexico (34.5°N, 104.2°W), on September 27, 1990, and September 25, 1993, and from Daggett, California (34.8°N, 114.8°W), on April 3, 1993. For the September 25, 1993, flight, vmr profiles were retrieved from infrared spectra obtained during payload ascent (near noon), as well as sunset and the following sunrise, providing the opportunity to measure the variations of NO and NO_2 during a daily solar cycle. Only sunset spectra were available for retrieval of vmr profiles for the other flights. An unapodized spectral resolution of 0.01 cm^{-1} was employed for tangent altitudes above ~28 km, at which point it was switched to 0.02 cm^{-1} to allow more rapid sampling, keeping the tangent point separation of successive spectra in the 2–3 km range. All flights of the MkIV were accompanied by an in situ O_3 UV photometer. The submillimeter limb sounder (SLS) instrument, which measures ClO, HCl, HO_2, and O_3 between altitudes of 35 and 50 km by microwave emission spectrometry [*Stachnik et al.*, 1992], flew on the same gondola for the April and September 1993 flights. The Far Infrared Limb Observing Spectrometer (FILOS), which measures OH between 35 and 45 km by submillimeter spectroscopy [*Pickett and Peterson*, 1993], accompanied the MkIV on the September 1993 flight.

3. Data Analysis

The MkIV data analysis consists of two distinct procedures, which are described further by *Sen et al.* [1996]. Briefly, nonlinear least squares fitting is first used to calculate the line of sight column abundance for each target gas in every spectrum. For gases that absorb in more than one spectral interval a weighted average column is calculated. These line of sight columns, together with the matrix of computed geometrical line of sight distances, are then solved to yield vmr profiles. At sunrise and sunset the tangent point separation varies from ~1 km near the balloon to typically 2–3 km at lower altitudes. The vmr profiles were retrieved on a 1 km vertical grid to maintain the high vertical resolution of the profiles immediately below the balloon and also of the ascent profiles, for which the vertical separation between successive spectra was typically only 0.9 km.

The molecular parameters are taken from the Atmospheric Trace Molecule Spectroscopy (ATMOS) experiment line list compilation based on the High Resolution Transmission Molecular Absorption Database (HITRAN) and updated with new spectroscopic measurements [*Brown et al.*, 1996]. The line list incorporates the latest laboratory cross sections for N_2O_5 [*Cantrell et al.*, 1988], HNO_4 [*May and Friedl*, 1993], and $ClNO_3$ [*Bell et al.*, 1992]. The estimated uncertainties in the accuracy of the line list parameters used for NO_y gas retrievals range from 8% to 10% for NO and NO_2, 15% for $ClNO_3$, HNO_3, and N_2O_5, and 20% for HNO_4 [*Brown et al.*, 1996]. The uncertainties for O_3 and N_2O are each ~5%.

The errors in the vmr profiles reported here represent the 1σ measurement precision combined in quadrature with the spectroscopic accuracies described above. Other systematic error terms such as pointing and temperature uncertainties are negligible: pointing errors have been minimized by fitting temperature insensitive CO_2 lines, and temperature errors have been minimized by using temperature sensitive CO_2 lines. Independent retrievals of the vmr profile of N_2 confirm that the viewing geometry and atmospheric conditions (pressure and temperature) have been calculated accurately. The measurement precision is calculated during the retrieval process based on considerations such as residuals in spectral fitting. In general, gases with numerous, strong, well-isolated spectral lines (e.g., O_3, NO, NO_2, and HNO_3) yield precisions in their retrieved vmr of typically ~5% of the peak vmr. *Abrams et al.* [1996] report similar uncertainties in the accuracy of gases measured by ATMOS, also obtained using high-resolution infrared solar occultation spectra.

For NO and NO_2, whose concentrations vary along the line of sight because of the changing solar zenith angle, diurnal correction matrices were calculated using the photochemical model described below for conditions (e.g., temperature and O_3) appropriate for each occultation. Figure 1 compares profiles of NO and NO_2 retrieved with (solid line) and without (dashed line) these diurnal corrections. The large fractional variations of NO at sunset result in significant differences be-

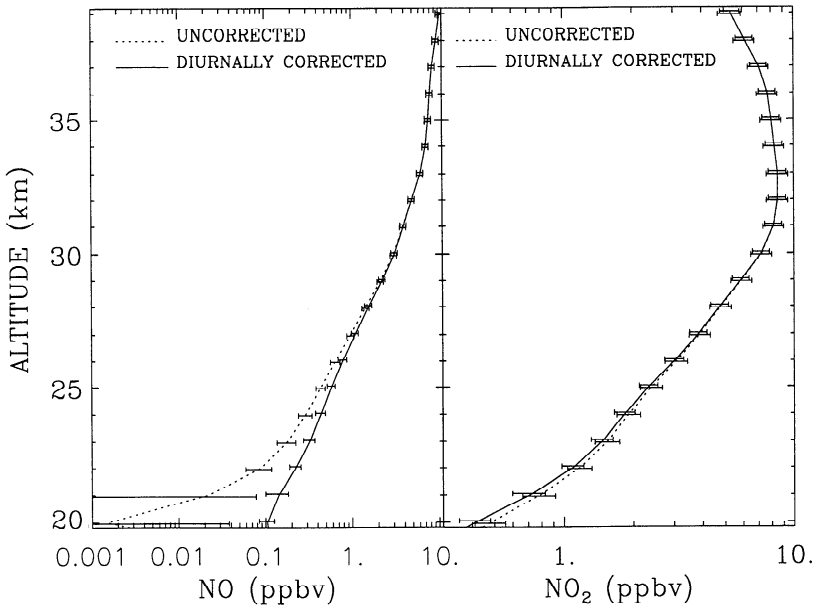

Figure 1. MkIV measurements of volume mixing ratio (vmr) profiles of NO and NO_2 at sunset on September 25, 1993, retrieved with and without diurnal corrections (see text). Error bars have been displaced in altitude slightly for visual clarity.

tween its two profiles, especially below 25 km. However, for NO_2, whose fractional variation at sunset is smaller, the diurnally corrected vmr is ~10% less than the uncorrected vmr at 20 km, with progressively smaller differences at higher altitudes. These results are in accordance with previous work on diurnal corrections [*Boughner et al.*, 1980; *Roscoe and Pyle*, 1987; *Russell et al.*, 1988]. The elements of these correction matrices are simply ratios of calculated concentrations at different solar zenith angles and altitudes. Therefore the absolute values of model concentrations are not communicated to the retrieval algorithm and do not bias the retrieved profiles. Since good agreement is achieved between in situ measurements of the relative variation of NO and NO_2 near the terminator and our photochemical simulations [*Salawitch et al.*, 1994b; *Newchurch et al.*, 1996], we believe that for NO_2, and for NO above 25 km, the diurnal corrections are not a significant source of uncertainty. The good agreement between diurnally corrected profiles for NO from 18 to 20 km measured by ATMOS and colocated in situ measurements of NO suggests the diurnal correction procedure can yield accurate retrievals at altitudes as low as 18 km [*Newchurch et al.*, 1996].

4. Photochemical Model

The photochemical model has been used previously in many stratospheric studies [e.g., *McElroy et al.*, 1992]. Reaction rates and absorption cross sections were adopted from the JPL 94-26 compendium [*DeMore et al.*, 1994]. The abundance of radical (i.e., NO, NO_2, OH, HO_2, ClO, and BrO) and reservoir (i.e., HNO_3, HCl, N_2O_5, and $ClNO_3$) gases has been calculated allowing for diurnal variation and assuming a balance between production and loss rates of each species integrated over a 24 hour period, for the latitude and temperature of the observations. Concentrations of precursors (i.e., O_3, H_2O, CH_4, CO, and C_2H_6), the total abundance of NO_y, and Cl_y (~HCl + ClO + HOCl + $ClNO_3$) are constrained to match observations of MkIV and SLS, which measured ClO from the same gondola. The temperature profile was obtained from the MkIV analysis of temperature sensitive CO_2 absorptions and for September 1993 equaled 216, 222, and 230 K at 22, 26, and 32 km, respectively. The input O_3 profile is based on observations by MkIV, SLS, and an in situ O_3 UV photometer (Plate 1) and is discussed in detail by *Osterman et al.* [1997].

All heterogeneous reactions on sulfate aerosols believed to affect partitioning of stratospheric NO_y and Cl_y at midlatitudes were included in the model. Heterogeneous hydrolysis of N_2O_5 was assumed to occur with a reaction probability of 0.1 [*DeMore et al.*, 1994]; the formulation of *Hanson et al.* [1996] was used for the heterogeneous rate of $BrNO_3$ + H_2O; and the formulations of *Ravishankara and Hanson* [1996] were used for the sulfate heterogeneous reactions HCl + $ClNO_3$, HOCl + HCl, and $ClNO_3$ + H_2O. Kinetic parameters used for the heterogeneous reaction of HOBr + HCl are from *Hanson and Ravishankara* [1995]. Profiles of aerosol surface area originated from zonal, monthly mean observations of SAGE II [*Yue et al.*, 1994].

5. Results and Discussion

Accurate measurements of ozone are a prerequisite for quantifying our understanding of nitrogen oxides. Not only does O_3 directly affect the NO/NO_2 and NO_2/HNO_3 ratios, but it also influences many other radicals (e.g., ClO and OH) that interact with NO_x and NO_y. Plate 1 shows a comparison of the sunset profile of ozone measured by MkIV on September 25, 1993, and ascent and descent profiles observed by the in situ O_3 UV photometer on board the same gondola. The two in situ measurements of O_3, obtained ~20 hours apart and separated by 200 km, agree to better than 5%. The excellent agreement between the in situ and remote observations of O_3, better than 6% for altitudes above 20 km, provides confidence that the O_3 profile is not a major source of uncertainty in the model calculations of the apportionment of nitrogen oxides into member

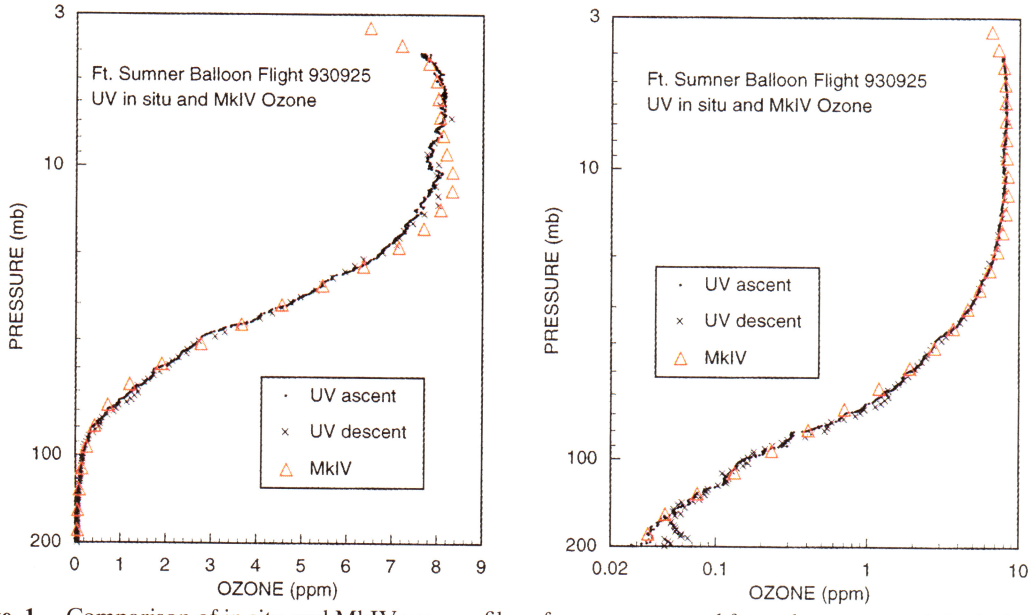

Plate 1. Comparison of in situ and MkIV vmr profiles of ozone measured from the same gondola during the September 25, 1993, balloon flight. The MkIV profile was measured at sunset. The in situ O_3 UV photometer measured profiles during ascent and during descent, which occurred on the following day. The data are identical on both panels, which have been chosen to highlight comparisons of different height regimes.

ecies. Since all the gases measured by MkIV are analyzed h the same spectral fitting and retrieval algorithms, the good eement for O_3 and also for N_2 lends confidence that the er gases, for which no direct validation is possible, are also ieved accurately. The excellent agreement between ATMOS (using a measurement and data analysis technique similar to MkIV) and in situ measurements of N_2O, CH_4, H_2O, NO_y, O_3, CFC-11, CFC-12, CCl_4, and SF_6 further demonstrates the accuracy achievable by the solar occultation technique [*Chang et al.*, 1996a, b].

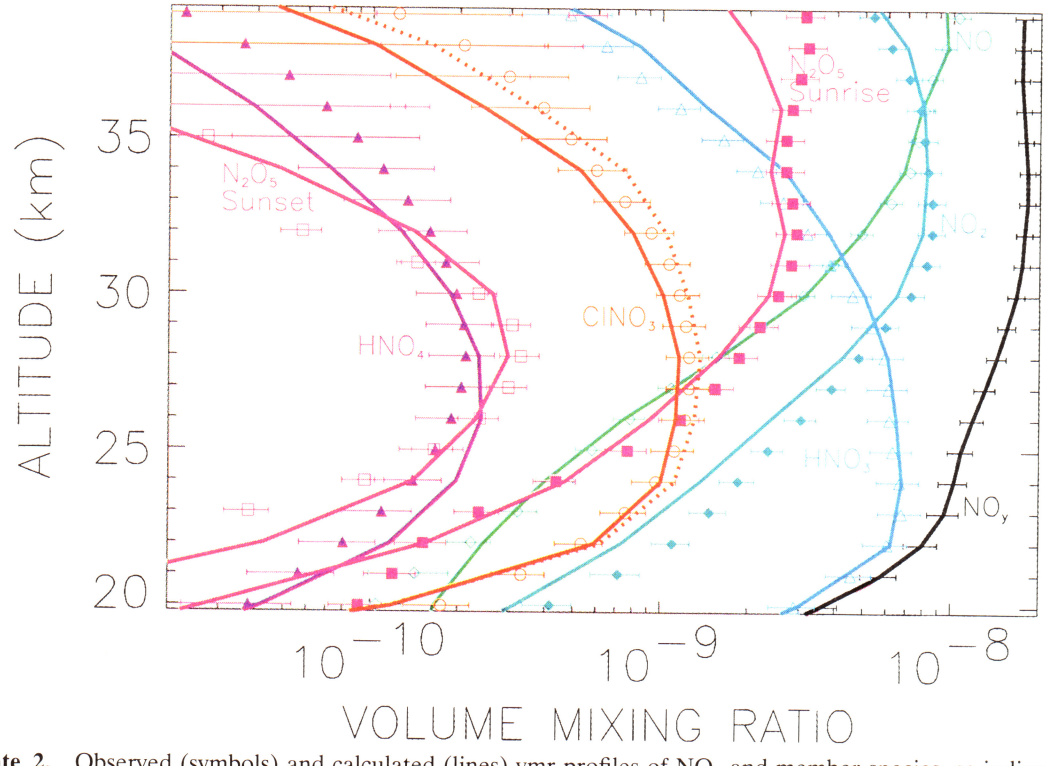

Plate 2. Observed (symbols) and calculated (lines) vmr profiles of NO_y and member species, as indicated, for sunset at 35°N on September 25, 1993. Sunrise profiles for N_2O_5 are also shown. The NO_y profile represents the sum of nitrogen oxides measured by MkIV and is used to constrain the model (see text). Calculated curves for $ClNO_3$ are shown for the 0% (dotted line) and 7% (solid line) yields of HCl from ClO + OH.

5.1. NO_y Partitioning and Budget

Observed and theoretical vmr profiles of NO_y species at sunset are illustrated in Plate 2. Profiles for N_2O_5 at sunrise are also shown. Calculated profiles of NO_y species not observed by MkIV (NO_3, $BrNO_3$, and HNO_2) make only small contributions to the total budget and are therefore not shown. Overall, the agreement between observed and calculated profiles for all NO_y species is typically better than 10%. The only significant systematic disagreement is for NO_2 below 28 km, where measured values exceed calculated values by up to 30%. Consequently, the observed ratios NO_2/NO and NO_2/HNO_3 exceed theoretical estimates below 28 km. The disagreement between observed and modeled NO at 20 km could result from an imperfect diurnal correction, which is not included in our estimate of the error bars.

The comparisons shown in Plate 2 demonstrate good understanding of most reactive and photolytic processes that regulate the abundance of nitrogen oxides, particularly for altitudes above 28 km. The observed buildup of N_2O_5 during the night as well as its value at the evening terminator are simulated accurately, suggesting the coupling between NO_x and HNO_3 is being treated in a realistic manner by the model. The range of altitudes for which NO, NO_2, and HNO_3 are calculated to be the dominant species of the NO_y family agrees with observations, as does the concentration of each gas for these altitudes. This suggests that the height dependence of the concentration of atomic oxygen and the photolysis rate of NO_2 are represented accurately by the model above 28 km and the production and loss processes for HNO_3 are represented accurately at lower altitudes. The proper treatment of HO_x above 28 km is supported by the agreement between observed and theoretical profiles of NO_2 and HNO_4 (produced by the reaction of NO_2 with HO_2), as well as comparisons with vmrs of OH and HO_2 observed by different instruments from the same gondola [*Pickett and Peterson*, 1996; *Osterman et al.*, 1997].

Two simulations of $ClNO_3$ are illustrated in Plate 2. The nominal case (solid line) assumes a 7% yield of HCl from ClO + OH and the *Michelsen et al.* [1994] formulation for the quantum yield of $O(^1D)$ from photolysis of O_3, while the other (dashed line) assumes a 0% HCl yield and the *DeMore et al.* [1994] formulation of the $O(^1D)$ quantum yield. Only the nominal case is shown for simulations of other species since calculated profiles are insensitive to the choice of these two kinetic parameters. The vmr profile of $ClNO_3$ observed by MkIV generally lies between the two theoretical calculations. A 7% yield of HCl is consistent with (1) ATMOS observations of HCl and $ClNO_3$ [*Michelsen et al.*, 1996], (2) Far-Infrared Spectrometer 2 (FIRS 2) measurements of HCl and HOCl obtained on September 26, 1989 [*Chance et al.*, 1996], and (3) SLS measurements of ClO during the September 1993 balloon flight [*Osterman et al.*, 1997]. While the MkIV measurements are not inconsistent with a 7% yield of HCl, they do suggest a smaller yield for reasons not fully understood [*Jaeglé*, 1995].

The photochemical model simulations shown in Plate 2 have been constrained to match the total amount of NO_y measured by MkIV at each altitude, as discussed above in section 4. MkIV also obtains simultaneous measurements of the concentration profile of N_2O, the source of NO_y. Figure 2 illustrates the correlation between NO_y and N_2O observed by MkIV, as well as the correlation measured by in situ instruments aboard the ER-2 aircraft at northern midlatitudes during February and November 1994. The in situ determination of NO_y is

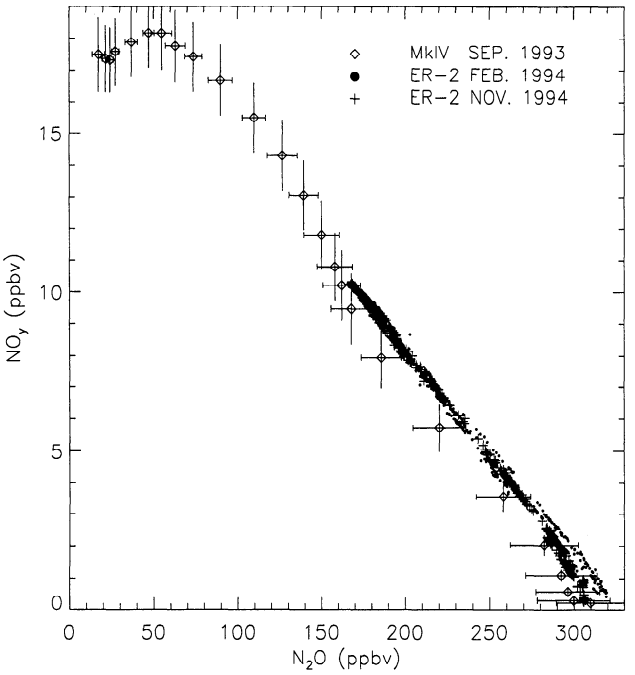

Figure 2. Correlation of the vmrs of NO_y (the sum of member species) and N_2O measured at sunset by MkIV (35°N; September 25, 1993) and measured by the National Oceanic and Atmospheric Administration (NOAA) (NO_y) and NASA Ames (N_2O) instruments aboard the ER-2 aircraft near 20 km (30°–40°N, February and November 1994).

ascribed a 1σ total uncertainty of better than 10% [*Fahey et al.*, 1989], while the in situ measurement of N_2O has an estimated 1σ total uncertainty of 3% [*Loewenstein et al.*, 1989]. Theoretically, NO_y and N_2O are expected to exhibit a compact, near-linear relation in the lower stratosphere since the timescale for redistribution by transport is short compared to photochemical production and loss of each quantity [*Plumb and Ko*, 1992]. The two measurements of NO_y versus N_2O agree to within the uncertainty of the observations: each is consistent with a slope of -0.07 for $160 < N_2O < 310$ ppbv, similar to two-dimensional model simulations [*Keim et al.*, 1997]. These comparisons corroborate the accuracy of the MkIV retrievals of the major NO_y species (e.g., HNO_3, NO_2, and NO) for the altitudes at which they are dominant. Furthermore, the MkIV observations illustrate the decrease of NO_y with decreasing N_2O at altitudes above 33 km because of the rapid (with respect to transport) loss of NO_y by the reaction of N + NO.

5.2. NO_x Chemistry

The reactions [*Crutzen*, 1970; *Johnston*, 1971]

$$NO + O_3 \rightarrow NO_2 + O_2 \quad (1)$$

$$NO_2 + O \rightarrow NO + O_2 \quad (2)$$

$$\text{Net: } O_3 + O \rightarrow 2 \cdot O_2 \quad (3)$$

constitute the primary chemical loss process for stratospheric ozone between altitudes of ~24–36 km [e.g., *Jucks et al.*, 1996; *Osterman et al.*, 1997]. Understanding the processes that regulate NO, NO_2, and NO_x is central to understanding the chemistry of stratospheric O_3. Loss of NO occurs primarily by (1), with a small contribution from

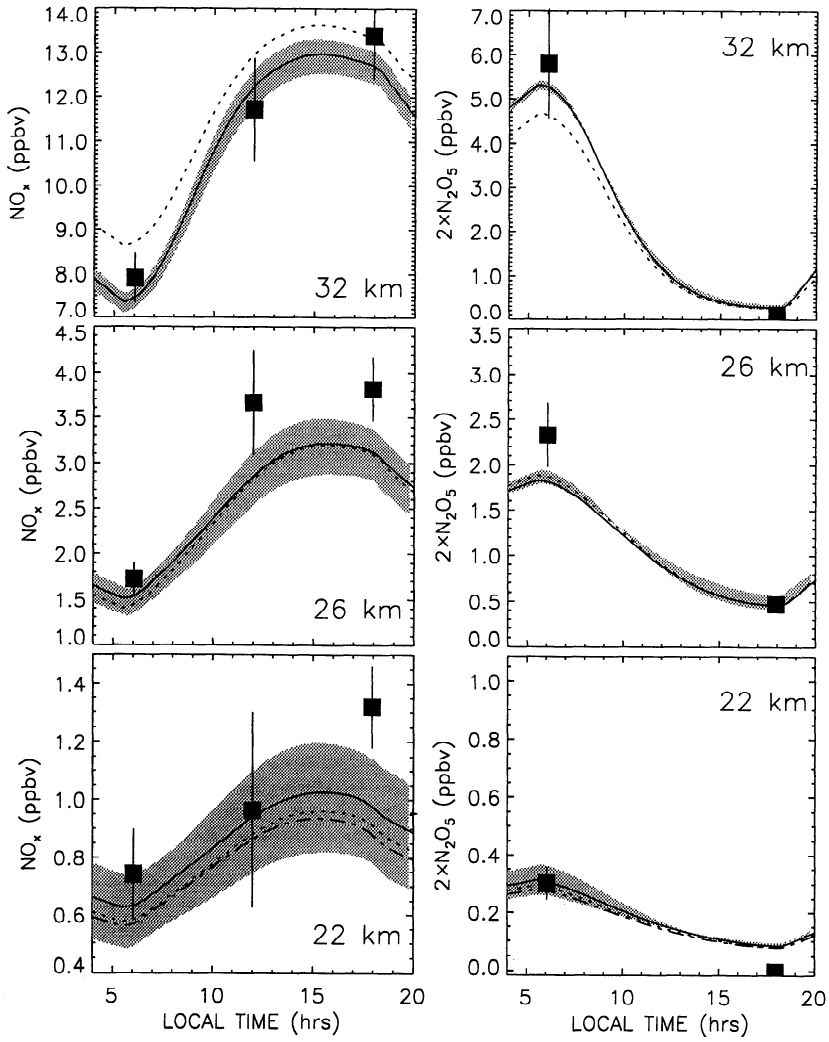

Figure 3. Comparison of observed and calculated diurnal variation of NO_x and N_2O_5. The shaded region illustrates the sensitivity of calculated NO_x and N_2O_5 to variations in albedo, subject to constraints for precursors measured by MkIV at sunset (solid line) and sunrise (dotted line). The dash-dotted line shows the model calculations of NO_x and $2{\cdot}N_2O_5$ for 22 km, using the value of J_{NO_2} that reproduces the measured NO/NO_2 ratio at sunset.

$$NO + ClO \rightarrow NO_2 + Cl \quad (4)$$

Removal of NO_2 occurs mainly by

$$NO_2 + h\nu \rightarrow NO + O \quad (5)$$

which is much faster than loss by (2) for altitudes below 35 km. Since the interconversion between NO and NO_2 occurs rapidly, the ratio of the concentration of these species is expected to be described by the instantaneous value of

$$\frac{NO}{NO_2} = \frac{J_{NO_2}}{k_1[O_3] + k_4[ClO]} \quad (6)$$

where J_{NO_2} is the photolysis rate of NO_2 and k_1 and k_4 are rate constants for the respective reactions.

Changes in NO_x occur much more slowly than the time for equilibration of NO and NO_2. Removal of NO_x occurs mainly by production of N_2O_5 and HNO_3:

$$NO_2 + O_3 \rightarrow NO_3 + O_2 \quad (7)$$

$$NO_3 + NO_2 + M \rightarrow N_2O_5 + M \quad (8)$$

$$N_2O_5 + H_2O\ (\text{sulfate}) \rightarrow 2 \cdot HNO_3 \quad (9)$$

$$NO_2 + OH + M \rightarrow HNO_3 + M \quad (10)$$

Resupply of NO_x occurs primarily by photolysis of N_2O_5 and HNO_3 and reaction of HNO_3 with OH. Between altitudes of 26 and 40 km, changes in the concentrations of NO_x and N_2O_5 between sunrise and sunset are expected to exhibit a 2:1 stoichiometry because N_2O_5 is the dominant nighttime reservoir of NO_x. At lower altitudes the stoichiometry is expected to exceed 2:1 because of the slight diurnal variation in the concentration of HNO_3.

MkIV observations of NO_x and N_2O_5 test our understanding of the diurnal variation of reactive nitrogen. Measured concentrations of NO_x and $2{\cdot}N_2O_5$ at sunrise and sunset for three altitudes are shown in Figure 3. Also shown are midday measurements of NO_x obtained during balloon ascent and retrieved using the same procedures as the sunset and sunrise profiles taking into account the fundamental difference in observation geometry. The midday profile of N_2O_5 could not be

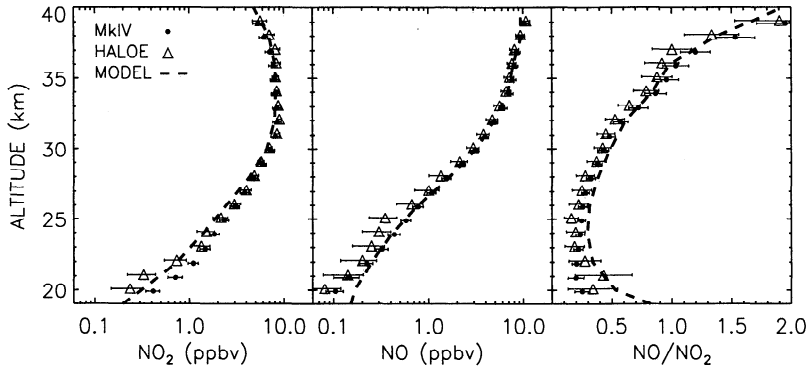

Figure 4. Halogen Occultation Experiment (HALOE) (triangle; version 18; 33.6°N, 110°W; September 24, 1993) and MkIV (circle; 34.5°N, 108°W; September 25, 1993) measurements of NO, NO_2, and the NO/NO_2 ratio at sunset. The measurements have been displaced in altitude slightly for visual clarity of the error bars. Model profiles of NO, NO_2, and the NO/NO_2 ratio are included for comparison.

retrieved since the air mass was too small to provide sufficient absorption in the ascent spectra.

Theoretical curves for the diurnal variation of NO_x and N_2O_5 are shown also in Figure 3. The curves are results of independent simulations constrained by measured concentrations of precursors at sunset (solid line) and sunrise (dotted line), assuming a cloud-free atmosphere with an albedo of 0.24. The shaded region indicates the sensitivity of model results to variations in albedo: highest values of NO_x are calculated assuming high altitude, highly absorbing clouds (albedo equal to 0.2), while lowest values are found assuming highly reflecting clouds (albedo equal to 0.8). Changes in albedo were allowed to impact all photolytic processes (e.g., J_{NO_2}, which affects the NO/NO_2 ratio on rapid timescales, as well as J_{HNO_3}, which affects NO_x/HNO_3 on longer timescales) and is meant to quantify, in a simple manner, the uncertainty of model results associated with the photolytic environment experienced by air parcels during the period of observation as well as the days immediately prior. The atmosphere was cloud-free in the MkIV field of view when the sunset spectra were obtained (spectra were recorded for tangent heights as low as 6 km), but contained high-altitude thunderstorm clouds during sunrise.

The results shown in Figure 3 demonstrate a fundamentally good understanding of the coupling between stratospheric NO_x and N_2O_5. Observed values of NO_x and N_2O_5 agree with theory at 32 km to within the measurement and model uncertainties. Similarly, observed values of NO_x at sunrise and N_2O_5 at sunset for 26 km agree with model values. However, at this altitude, observations of NO_x at both midday and sunset as well as N_2O_5 at sunrise exceed model values, although theory and observation overlap slightly given the respective uncertainties. MkIV observations of variations in concentrations of NO_x and N_2O_5 at both 26 and 32 km exhibit the expected 2:1 stoichiometry. During sunset at 22 km, observations of NO_x exceed theory, and N_2O_5 is less than theory, by amounts roughly consistent with the expected stoichiometry.

The only significant discrepancy in this study is the tendency of observed NO_2 to exceed model values below 28 km (e.g., Plate 2). The strong and well-defined infrared absorptions of NO_2 make it one of the more easily measured gases in the MkIV spectra. Two separate bands at 1600 and 2900 cm^{-1} are used to retrieve NO_2, and the resulting profiles are consistent to better than 10% for all altitudes and to better than 5% below 27 km. The profile of NO_2 shown in Plate 2 is a weighted average of retrievals from both bands. The good agreement between measured and calculated NO_2 above 30 km, where pressure broadening of the NO_2 absorption features is negligible, indicates that errors in the NO_2 line strengths are unlikely to be the cause of the discrepancy at lower altitudes. Recent measurements of the NO_2 pressure-broadened half widths (PBHW) in the 2900 cm^{-1} band [*Dana et al.*, 1997] indicate the values in the HITRAN and ATMOS line lists used in this study may be up to 20% too small. Our preliminary analysis of unpublished spectra of the 1600 cm^{-1} NO_2 band (D. Newnham, Rutherford-Appleton Laboratory, personal communication, 1997) indicate that the widths of these lines are also too small in the HITRAN and ATMOS line lists. Test retrievals based on the recently published half widths indicate an ~10% decrease in the vmr of NO_2 measured at 25 km, with little effect above 30 km. We are reluctant, however, to formally adopt these revisions into our retrievals of NO_2 until they have been confirmed by further laboratory measurements and incorporated into the HITRAN line list. Therefore the spectral parameters used here are consistent with those used by ATMOS and HALOE.

Our estimate of the total uncertainty of the MkIV measurements of NO_2 varies from 19% at 20 km to 11% at 30 km. Uncertainties in the strengths and PBHW of the NO_2 lines dominate these values. Therefore, the discrepancy between observations and theory is significant below 28 km. Additionally, NO and HNO_3 are measured with sufficient accuracy and precision in the lower stratosphere that the discrepancy between theory and observations of the NO/NO_2 and NO_2/HNO_3 ratios are also larger than the measurement uncertainty below 28 km.

Figure 4 illustrates measurements of NO, NO_2, and their ratio by HALOE (version 18; 33.6°N, 110°W) made 24 hours earlier and 200 km distant from the MkIV observations on September 25, 1993. The HALOE measurements of NO are based on absorption in the 1900 cm^{-1} band, identical to that used by MkIV. The HALOE measurements of NO_2 are based on absorption in the 1600 cm^{-1} band, one of the two bands used in the MkIV analysis. The estimated total uncertainties of individual retrievals of NO and NO_2 by HALOE are 40% and 26%, respectively, at 22 km [*Gordley et al.*, 1996, Figures 7 and 8]. The two remote measurements of NO, NO_2, and their ratio agree to within 12% above ~25 km. The calculated profiles describing MkIV sunset measurements are reproduced for

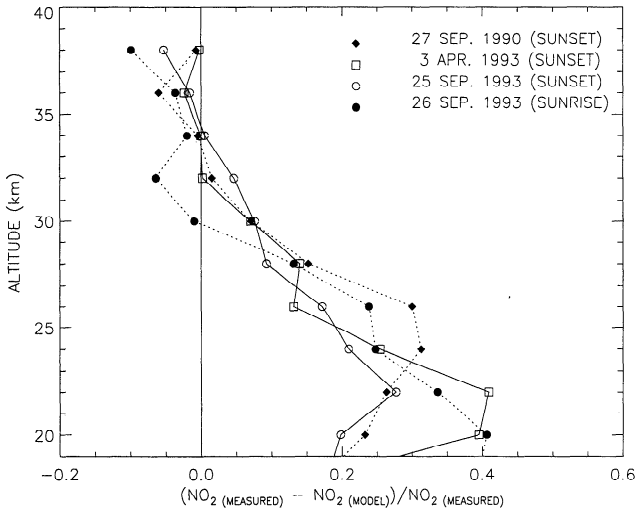

Figure 5. The fractional difference between measured and calculated NO_2 for September 1990, April 1993, and September 1993 balloon flights of the MkIV. Model simulations were constrained by MkIV measurements of precursors appropriate for each flight.

comparison purposes. Between 23 and 34 km the MkIV and HALOE measurements of NO_2 are both larger than the model values. Below 23 km the progressively larger uncertainties associated with the measurements make it difficult to draw definitive conclusions.

The disagreement between NO_2 measured by MkIV and the calculated values exhibits a similar pattern with respect to altitude for all balloon flights analyzed to date, as shown in Figure 5. These flights sampled air with substantially different levels of aerosol loading, reflecting the relatively clean period prior to the eruption of Mount Pinatubo and the resulting enhancement and subsequent decline of volcanic aerosol. This suggests the NO_2 discrepancy is not related to transient phenomena such as the possible effect of Mount Pinatubo aerosol on the photolysis rate of NO_2. Recent ATMOS measurements obtained in November 1994 at high southern latitudes with relatively low aerosol loading reveal a similar pattern of excess NO_2 with respect to model profiles [*Rinsland et al.*, 1996, Figure 3]. Similarly, an analysis of UARS and SAGE II observations shows consistently higher values of the measured NO_x/NO_y ratio than expected in the lower stratosphere during periods of moderate aerosol loading [*Morris et al.*, 1997, Plate 1]. Nighttime measurements of NO_2 obtained by UV-visible spectroscopy in March 1994 at 44°N latitude also exceed calculated values in the 22–28 km altitude range [*Renard et al.*, 1997]. However, an analysis of earlier ATMOS observations obtained at midlatitudes during April/May 1985 does not reveal a similar discrepancy for NO_2 [e.g., *McElroy et al.*, 1992, Figures 10 and 12].

Figure 6 illustrates the variation with respect to solar zenith angle of MkIV observations of NO, NO_2, and the NO/NO_2 ratio at altitudes of 32, 26, and 22 km. The model simulations are similar to those shown in Figure 3, for sunset (solid line) and sunrise (dotted line) constraints and a cloud-free albedo of 0.24. The shaded regions represent the sensitivity of calculated values to variations in albedo, as discussed previously. The observed concentrations of NO agree with theory, to within the measurement and model uncertainty, at all altitudes and times except for 26 km at sunrise. However, the precision of the midday observations of NO is poor below 26 km owing to the low air mass factor of the ascent spectra. Similarly, the noontime measurements of NO_2 below 27 km are not sufficiently accurate or consistent to ascertain whether they agree better with the model or with the 20–30% excess over model values at sunrise and sunset.

The observed NO/NO_2 ratio is lower than model values at sunrise and sunset for altitudes below 26 km (Figure 6). Calculated photolysis rates of NO_2 agree well with those inferred from observations of the direct and diffuse flux of radiation between 300 and 775 nm obtained aboard the ER-2 aircraft [*McElroy et al.*, 1995] for solar zenith angles as high as 80° at 20 km [*Gao et al.*, 1997, Figure 4]. Therefore the photolysis rate of NO_2 is unlikely to cause the discrepancy in NO/NO_2 ratio illustrated in Figure 6. Since loss of NO at 22 km by reaction with O_3 proceeds at a rate ~4 times faster than loss by reaction with ClO and theory and observation of ClO are in reasonable agreement [*Avallone et al.*, 1993; *Salawitch et al.*, 1994a; *Chang et al.*, 1996a], it is unlikely that uncertainties in the kinetics of (4) or in the abundance of ClO will resolve the dilemma posed by the observations of NO/NO_2.

Figure 7 illustrates the recommended value for the rate constant of the reaction NO + O_3 from the JPL compendium, as well as its nominal 1σ uncertainty [*DeMore et al.*, 1994], as a function of inverse temperature. Also shown are individual laboratory measurements used in the determination of the recommended rate. The recommended uncertainty of the rate is ~50% for a temperature of 220 K [*DeMore et al.*, 1994], considerably larger than the standard deviation about the mean of the individual measurements at this temperature. Also shown is the rate for the reaction NO + O_3 required to balance, in the absence of any other kinetic changes, the NO/NO_2 ratio observed by MkIV at sunset. We do not intend to imply by this figure that rate constants can be determined from atmospheric measurements. It is merely a way of illustrating the uncertainty in the model calculation and its relationship to laboratory and atmospheric observations. The rate for NO + O_3 required to balance the observed NO/NO_2 ratio below 23 km is larger than is allowed by the laboratory observations, and consequently, uncertainties in this rate are an unlikely explanation for the observed ratio at the lowest altitudes. However, it is difficult to rule out the possibility, on the basis of individual laboratory measurements, that the true rate of (1) is 15% faster than the recommended value for temperatures near 216 K. Together with the revision of the NO_2 half widths described earlier, this would explain the measured NO/NO_2 ratios at sunrise and sunset between altitudes of 23 and 32 km.

This explanation would worsen the agreement between theory and in situ observation of NO (by chemiluminescence) and NO_2 (by chemiluminescence and by a tunable diode laser spectrometer) at midlatitudes obtained from the ER-2 aircraft. During the Stratospheric Photochemistry Aerosols and Dynamics Experiment (SPADE; May 1993) an ~35% discrepancy between theory and observation of the NO/NO_2 ratio near 20 km during midday was reported [*Jaeglé et al.*, 1994] but in the opposite sense of the discrepancy noted for the MkIV occultations. However, more recent measurements of NO and NO_2, obtained at midlatitudes near 20 km during the Airborne Southern Hemisphere Ozone Experiment/Measurements for Assessing the Effects of Stratospheric Aircraft (ASHOE/MAESA; February–November, 1994) using the in situ chemi-

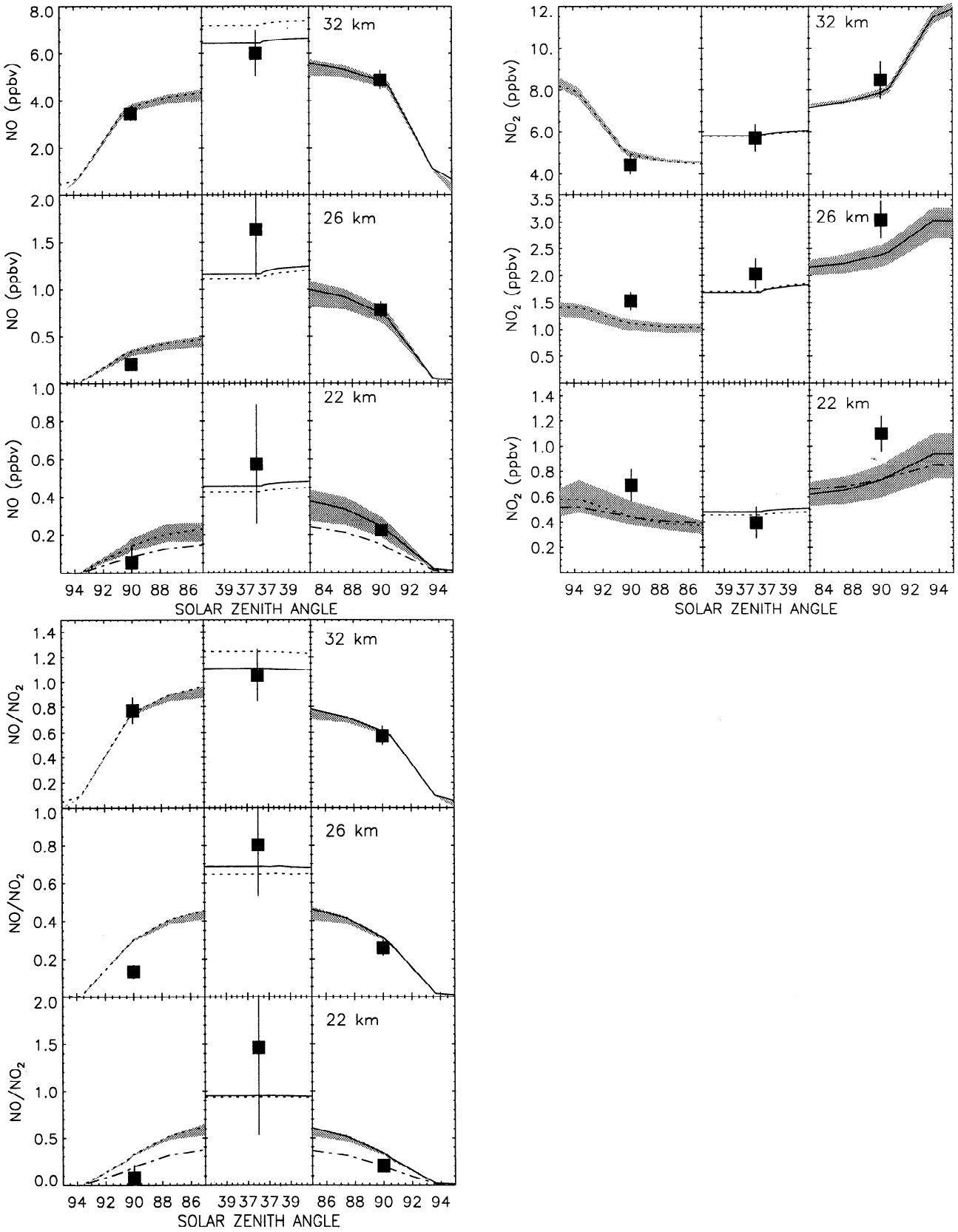

Figure 6. MkIV observations of NO, NO_2, and the NO/NO_2 ratio during (left) sunrise, (middle) midday, and (right) sunset on the September 1993 balloon flight for 22, 26, and 32 km (as indicated). Model curves represent the same simulations described in Figure 3.

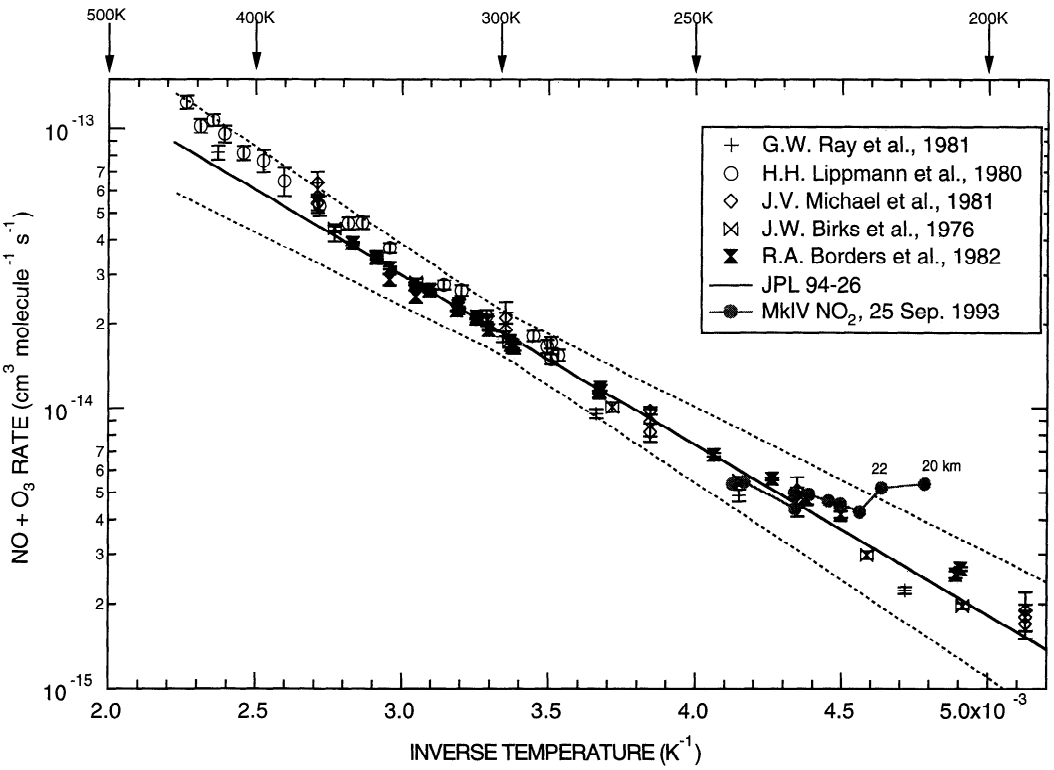

Figure 7. Measured and recommended rates of the reaction NO + O_3 → NO_2 + O_2. Recommended rate (solid line) and its range of uncertainty (dotted line) are from Jet Propulsion Laboratory (JPL) 94-26 [*DeMore et al.*, 1994] and are identical to values in the recently published JPL 97-4 compendium. Laboratory measurements (symbols) are shown with their respective uncertainties. Also shown is the rate of this reaction required to balance the NO/NO_2 ratio observed at various altitudes by MkIV at sunset on September 25, 1993 (shaded symbols).

luminescence detector, agree with the theoretical ratio to better than 8% [*Gao et al.*, 1997].

The MkIV observations suggest a deficiency in our understanding of the NO/NO_2 ratio. For illustrative purposes only we have calculated the abundance of NO_y gases at 22 km allowing for a 40% reduction in J_{NO_2} at all solar zenith angles, which forces agreement with the measured NO/NO_2 ratio. Results shown in Figure 6 indicate that even though the NO/NO_2 ratio is simulated correctly, the model values of both NO and NO_2 remain significantly lower than observation. Simultaneously matching constraints posed by MkIV observations of NO/NO_2 and NO_x/NO_y at 22 km requires not only a reduction in J_{NO_2} (or, equivalently, an increase in k_1) but also either a reduction in the rate of the heterogeneous hydrolysis of N_2O_5 (reaction (10)) from the recommended reaction probability of 0.1 [*DeMore et al.*, 1994] to a value as low as 0.02 or else accelerated removal of HNO_3.

Lary et al. [1997] have postulated that heterogeneous processes occurring on the surface of carbonaceous soot particles may convert HNO_3 to NO_2. Similarly, heterogeneous interaction of formaldehyde and HNO_3 on sulfate aerosol may also convert HNO_3 to NO_2 at warm temperatures [*Iraci and Tolbert*, 1997]. However, for stratospheric temperatures the effect of heterogeneous reactions involving formaldehyde on the NO_2/HNO_3 ratio has not been established. If these processes could act rapidly enough to compete with the loss of NO_x by (10), they would offer an explanation for the tendency of the MkIV observations of NO_2 to exceed model values. However, these reactions would cause serious difficulties in accounting for a wealth of observations of the NO/NO_y ratio obtained from the ER-2 [*Salawitch et al.*, 1994a, b; *Gao et al.*, 1997] as well as our observation of the NO/HNO_3 ratio above 22 km. Simultaneous measurements of NO, NO_2, and NO_y by instruments on the ER-2 and MkIV for the same air masses during the Photochemistry of Ozone Loss in the Arctic Region in Summer (POLARIS) campaign will hopefully shed additional light on our understanding of the processes that regulate NO_x.

5.3. The Effect of Mount Pinatubo Aerosols on NO_x

Increases by factors of 20–30 in the surface area of sulfate aerosol following the June 1991 eruption of Mount Pinatubo [e.g., *McCormick et al.*, 1995] led to reduced levels of NO_x throughout the stratosphere because of heterogeneous hydrolysis of N_2O_5 (reaction (10)) [e.g., *Fahey et al.*, 1993; *Webster et al.*, 1994]. The reduction in NO_x led to increases in concentrations of ClO and HO_x, increasing the overall efficiency of catalytic removal of O_3 in the lower stratosphere [e.g., *Rodriguez et al.*, 1991, *Kinnison et al.*, 1994]. Previous analyses of observations of NO and NO_y from the ER-2 [*Fahey et al.*, 1993; *Kawa et al.*, 1993; *Salawitch et al.*, 1994a, b; *Gao et al.*, 1997] suggest that (10) has been the dominant sink for NO_x throughout much of the lower stratosphere following the eruption of Mount Pinatubo. Similar conclusions were reached on the basis of analysis of balloon-borne observations of NO_2 and HNO_3 [*Webster et al.*, 1994] as well as NO and NO_y [*Kondo et al.*, 1997]. However, *Koike et al.* [1994] observed larger in-

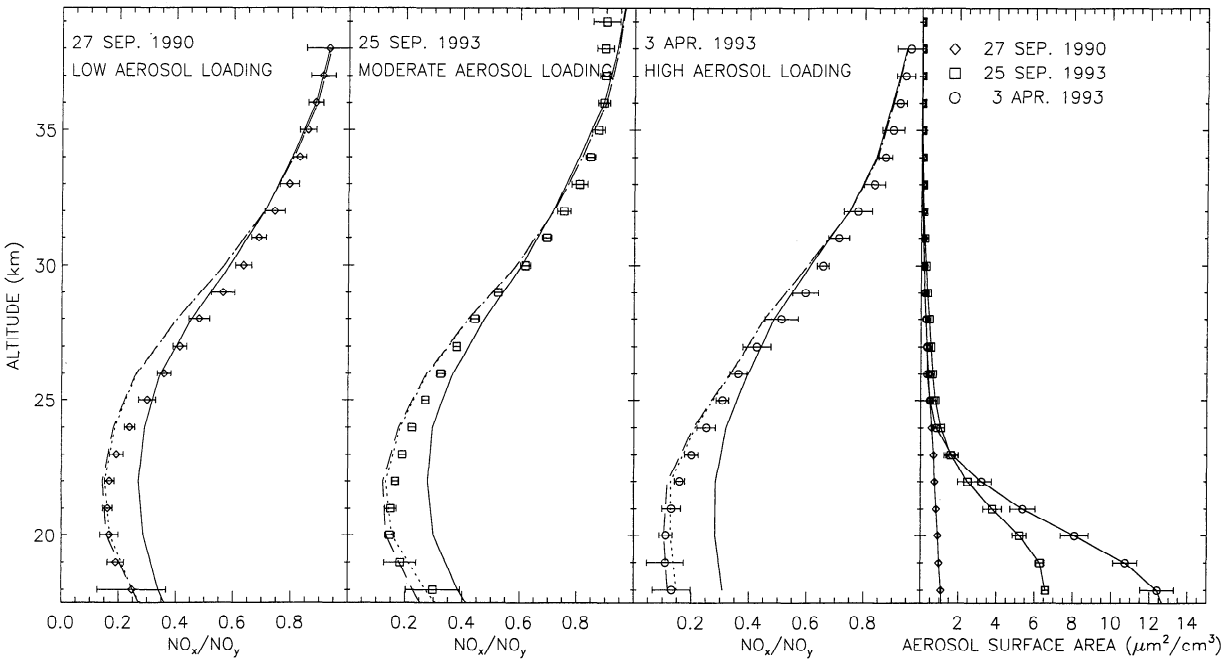

Figure 8. MkIV observations and calculated profiles of NO_x/NO_y as a function of altitude at sunset from three balloon flights at 35°N with differing levels of aerosol surface area are shown: pre-Mount Pinatubo eruption (September 1990), moderate recovery after the eruption (September 1993), and highly perturbed loading (April 1993). (right) Associated profiles of zonal, monthly mean aerosol surface area inferred from SAGE II extinction measurements are shown. Three simulations describe each balloon flight: (1) gas phase only (solid line), (2) gas phase and N_2O_5 hydrolysis (dotted line), and (3) gas phase and all heterogeneous reactions (dashed line). Each simulation was constrained by MkIV measurement of precursors for the appropriate flight.

creases in the column abundance of HNO_3, and decreases in column NO_2, than could be accounted for by (10) alone. The variation of in situ observations of HCl with aerosol surface area has been interpreted as evidence for a dominant influence by heterogeneous reactions involving HCl and $ClNO_3$ (Webster et al., submitted manuscript, 1997). Furthermore, *Solomon et al.* [1996] showed that the observed decline in O_3 during the past several decades, due to both the build up of chlorine from industrial CFCs and changes in sulfate aerosol loading, was about 50% larger than calculated by their two-dimensional model. Similarly, *Kinnison et al.* [1994] were unable to account for the magnitude of the observed reduction of O_3 following the eruption of Mount Pinatubo when both the radiative and chemical effects of volcanic aerosol were considered.

We present observations of NO, NO_2, and NO_y by MkIV for three balloon flights encountering vastly different levels of sulfate aerosol loading. These observations provide a test of our understanding of the heterogeneous chemistry associated with Mount Pinatubo aerosols on the NO_x/NO_y ratio. We seek to establish whether the observations provide evidence that heterogeneous sinks of NO_x other than (10) exert a substantial influence on the chemistry of the midlatitude stratosphere. If so, loss of O_3 due to Mount Pinatubo aerosols would likely exceed model predictions [e.g., *Prather*, 1992].

Figure 8 compares the measured profiles of NO_x/NO_y at sunset to theoretical profiles for flights of the MkIV during September 1990, April 1993, and September 1993. Also shown are the profiles of the sulfate aerosol surface area associated with each MkIV flight, derived from SAGE II zonal, monthly mean measurements of extinction in the visible and near ultraviolet [*Yue et al.*, 1994]. The theoretical curves for NO_x/NO_y are constrained by profiles of O_3, H_2O, CH_4, NO_y, and HCl + $ClNO_3$ + HOCl, temperatures measured by MkIV for each flight, and the SAGE II surface area profiles shown in Figure 8. Three model curves for NO_x/NO_y are shown for each flight: results of (1) a purely gas phase calculation (solid line), (2) gas phase plus N_2O_5 hydrolysis (reaction (10)) only (dotted line), and (3) gas phase plus all heterogeneous reactions (dashed line). Calculated values of the NO_x/NO_y ratio are nearly identical for the two heterogeneous simulations because temperatures encountered during the three flights were too warm (209, 211, and 209 K at 20 km for September 1990, April 1993, and September 1993, respectively) and aerosol surface areas were too low for substantial loss of NO_x by the two heterogeneous reactions involving $ClNO_3$ [e.g., *Ravishankara and Hanson*, 1996]. The small difference between the two heterogeneous simulations is predominantly due to the reaction of $BrNO_3$ + H_2O. This reaction does not become an efficient sink of NO_x for levels of aerosol loading encountered during April 1993 and contemporary levels of Br_y [e.g., 17.9 pptv at 22 km for April 1993] until air parcels reach latitudes poleward of 50°, where the less intense photolytic environment leads to slower rates for competing processes [*Tie and Brasseur*, 1996].

The height dependence of the observed NO_x/NO_y ratio agrees fairly well with profiles calculated using the heterogeneous models, although the observed ratio exceeds theory between altitudes of 23 and 30 km. For this range of altitudes the observations agree more closely, in general, with the gas phase only calculations. For altitudes below 23 km, measured values of this ratio agree well with the heterogeneous simulations and

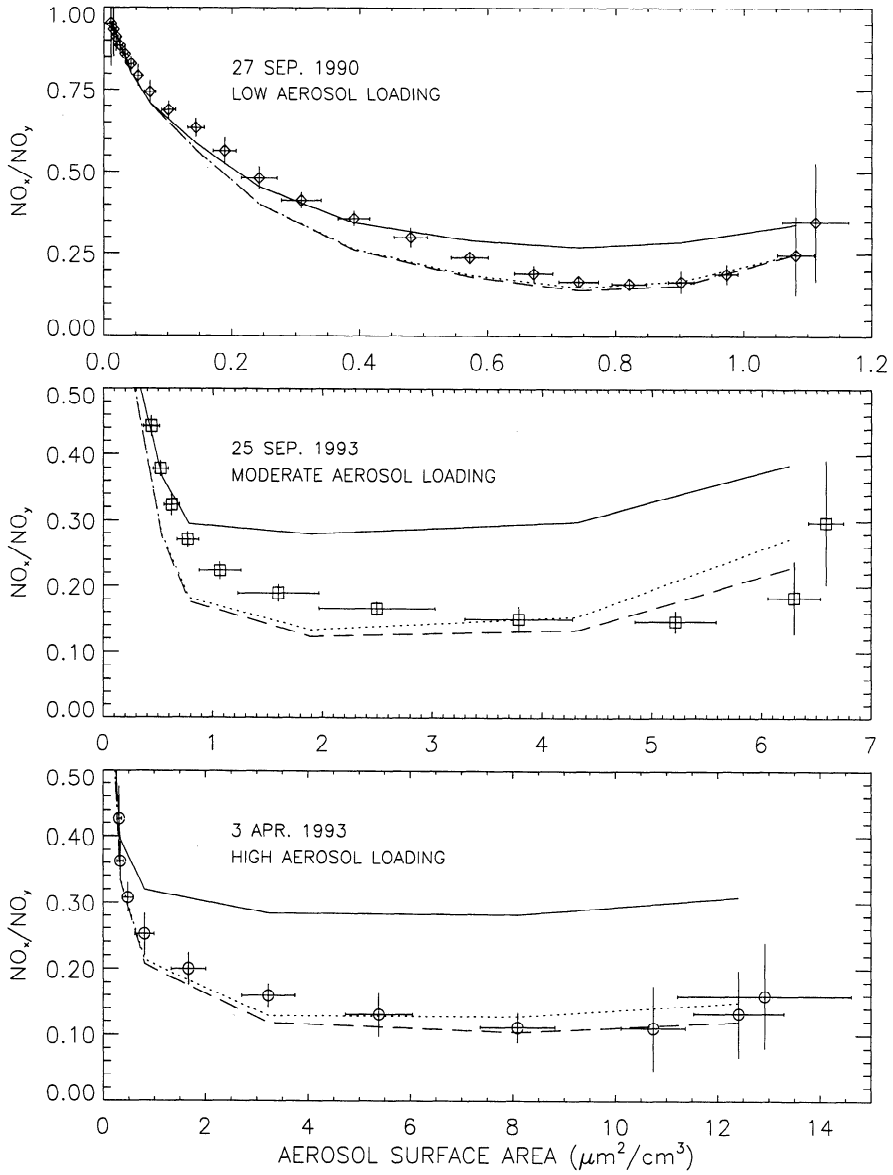

Figure 9. MkIV observations and calculated variation of NO_x/NO_y as a function of aerosol surface area for the three flights with varying degrees of aerosol loading described in Figure 8. Note changes in both abscissa and ordinate scale for the three panels. Model simulations are described in Figure 8.

are appreciably smaller than the gas phase only calculations, consistent with conclusions of numerous previous studies [e.g., *McElroy et al.*, 1992; *Dessler et al.*, 1993; *Fahey et al.*, 1993; *Webster et al.*, 1994; *Kondo et al.*, 1997].

It is tempting to contemplate the existence of a neglected process that converts HNO_3 to NO_x, such as heterogeneous reactions on soot as suggested by *Lary et al.* [1997], on the basis of the comparisons shown in Figure 8. Likewise, a large reduction in the rate of (10) would also yield better agreement between theory and observation of NO_x/NO_y between 23 and 30 km. However, the observation of excess NO_x relative to the heterogeneous model profiles is caused primarily by the discrepancy in NO_2, as discussed previously. The observed NO/HNO_3 ratio in this altitude range agrees well with profiles calculated using published rates for the heterogeneous reactions listed above (e.g., Plate 2). Furthermore, the heterogeneous model profiles of NO_x/NO_y agree with observed values below 23 km, even though the observed NO/NO_2 ratio is simulated poorly [e.g., Figure 6]. Understanding the cause of the discrepancy between theory and observation of the NO/NO_2 ratio, which should be in nearly instantaneous equilibrium with the value of (6), is a prerequisite for gaining further insight into the apparent disagreement for NO_x/NO_y between 23 and 30 km.

Figure 9 quantifies the dependence of the NO_x/NO_y ratio on aerosol surface area for the three flights. The model curves are identical to those shown in Figure 8. Aerosol surface area is used as the abscissa for all model results, even though it has no bearing on the gas phase simulation. The gas phase calculation captures the nonlinear dependence of the observed NO_x/NO_y ratio with increasing O_3, for aerosol surface area (a surrogate for both O_3 and altitude in Figure 9) values $<\sim 0.6\ \mu m^2\ cm^{-3}$, and consistently overpredicts the magnitude of the ratio at larger values of surface area. The abundance of O_3 controls both the apportionment of NO_x between NO and NO_2 and the nighttime formation of N_2O_5. Since the nighttime formation of

N_2O_5 occurs by the reaction of NO_2 and NO_3 (i.e., quadratically dependent on NO_x), the NO_x/NO_y ratio is expected to eventually become insensitive to increases in surface area beyond a critical value, provided $N_2O_5 + H_2O$ is the dominant sink for NO_x. The observations and calculations in Figure 9 suggest this critical value is ~4 μm^2 cm^{-3} for the conditions encountered during the balloon flights. This critical value and the NO_x/NO_y ratio at saturation are consistent with previous balloon and airborne chemiluminescence observations of NO and NO_y [*Dessler et al.*, 1993; *Fahey et al.*, 1993; *Kondo et al.*, 1997], suggesting $N_2O_5 + H_2O$ was the dominant sink of NO_x for the sampled air masses.

6. Conclusions

Volume mixing ratio profiles of numerous gases obtained at midlatitude (35°N) during the September 1993 balloon flight of the JPL MkIV interferometer and aerosol surface area based on SAGE II extinction measurements have been examined to assess our understanding of the NO_y budget and partitioning of NO_y species. The variation of the total nitrogen content (from the individual NO_y species) relative to N_2O agrees well with in situ observations and previously published relations found using two-dimensional models. The MkIV observations provide an important test for models since they extend to considerably higher altitudes than the in situ observations.

MkIV observations of NO, NO_2, and HNO_3 agree well with theoretical profiles for the range of altitudes over which each gas is the dominant NO_y species. Our observations of the diurnal variation of NO_x and N_2O_5 exhibit close agreement with the theoretical stoichiometry between 20 and 40 km, suggesting the coupling between NO_x and its dominant nighttime reservoirs is well understood. Measured vmr profiles of all NO_y species agree well with model profiles, except that the observed abundance of NO_2 in the lower stratosphere exceeds calculated values by 20–30%. The resulting discrepancies between theory and observation of the NO/NO_2 and NO_2/HNO_3 ratios for altitudes between 20 and 28 km are larger than the estimated total uncertainty (accuracy and precision) of the measurements. Published uncertainties in laboratory measurements of the absorption cross section of NO_2 and the rate of NO + O_3 [*DeMore et al.*, 1994] are individually smaller than the discrepancy for the NO/NO_2 ratio below ~23 km. However, a 15% increase in the rate of NO + O_3 at cold temperatures, together with a 10% increase in the pressure-broadened half widths of the NO_2 lines, would resolve the discrepancy between observation and theory of the NO/NO_2 ratio above 23 km and substantially improve the agreement at lower altitudes.

The comparison between theory and observation of the NO_x/NO_y ratio by the MkIV for balloon flights before (September 1990) and after (April and September 1993) the eruption of Mount Pinatubo suggests that N_2O_5 hydrolysis is the dominant heterogeneous sink of NO_x in the lower stratosphere for the conditions encountered. Additional heterogeneous reactions do not perturb this ratio appreciably for surface area below 14 μm^2 cm^{-3} for the temperatures (209–219 K) of our midlatitude observations. Our analysis of these observations suggests heterogeneous reactions involving $ClNO_3$ and HCl are not a significant sink for midlatitude NO_x, which had been a possible explanation for the quantitative anomalies of column NO_2 and HNO_3 presented by *Koike et al.* [1994]. The observed saturation of the NO_x/NO_y ratio limits the increase of ClO within the Cl_y reservoir. G. B. Osterman et al. (unpublished manuscript, 1997) show that MkIV observations of HCl and $ClNO_3$ at 20 km obtained during the same flights are relatively insensitive to surface area, providing further evidence that heterogeneous reactions involving $ClNO_3$ and HCl do not proceed rapidly enough to significantly alter NO_x or ClO for the sampled air masses. Our observations suggest the decline in reactive nitrogen by volcanic aerosol is well understood and that catastrophic loss of O_3 due to massive enhancements in ClO [e.g., *Prather*, 1992] and large reductions in HCl (Webster et al., submitted manuscript, 1997) is unlikely for the environmental conditions encountered by these balloon flights.

Note added in proof. Subsequent to submission of this paper, an updated JPL compendium of reaction rates and absorption cross sections was published [*DeMore et al.*, 1997]. The only significant difference between the updated kinetic parameters and those used here is the ~6% increase (for T = 220 K and $M = 2 \times 10^{18}$ cm^{-3}) in the rate constant for the reaction OH + NO_2 + M → HNO_3 + M. Adopting the updated rate would lower the calculated NO_x/HNO_3 ratio by 6%, 9%, and 15% at 22, 26, and 32 km, respectively. This change would slightly worsen the agreement between observed and calculated NO, NO_2, and HNO_3 at most altitudes but does not alter our overall conclusions.

Acknowledgments. The authors wish to thank D. C. Petterson, J. H. Riccio, R. D. Howe, and W. B. Wilson of JPL for their considerable field support during the balloon campaign. We wish to thank the NSBF which conducted the balloon launches, flight operations, and recovery of the payload. We also wish to thank D. W. Fahey (NOAA) for the use of the ER-2 NO_y data, M. Loewenstein (NASA Ames) for the use of the ER-2 N_2O data, and J. M. Russell III (Hampton University) for the use of the HALOE NO and NO_2 measurements. This work was funded by the NASA Upper Atmosphere Research Program and the NASA UARS Correlative Measurements Program. This research was performed at Jet Propulsion Laboratory, California Institute of Technology, under contract with the National Aeronautics and Space Administration.

References

Abrams, M. C., et al., On the assessment and uncertainty of atmospheric trace gas measurements with high-resolution infrared solar occultation spectra from space by the ATMOS experiment, *Geophys. Res. Lett.*, *23*, 2337–2340, 1996.

Avallone, L. M., et al., Balloon-borne in situ measurements of ClO and ozone: Implications for heterogeneous chemistry and midlatitude ozone loss, *Geophys. Res. Lett.*, *20*, 1795–1798, 1993.

Bell, W., G. Duxbury, and D. D. Stuart, High-resolution spectra of ν_4 band of chlorine nitrate, *J. Mol. Spectrosc.*, *152*, 283–297, 1992.

Birks, J. W., B. Shoemaker, T. J. Leck, and D. M. Hinton, Studies of reactions of importance in the stratosphere, 1, reaction of nitric acid with ozone, *J. Chem. Phys.*, *65*, 5181–5185, 1976.

Borders, R. A., and J. W. Birks, High-precision measurements of activation energies over small temperature intervals: Curvature in the Arrhenius plot for the reaction NO + O_3 → NO_2 + O_2, *J. Phys. Chem.*, *86*, 3295–3302, 1982.

Boughner, R. J., J. C. Larson, and M. Natarajan, The influence of NO and ClO variations at twilight on the interpretation of solar occultation measurements, *Geophys. Res. Lett.*, *7*, 231–234, 1980.

Brown, L. R., et al., The 1995 atmospheric trace molecule spectroscopy experiment (ATMOS) linelist, *Appl. Opt.*, *35*, 2828–2848, 1996.

Cantrell, C. A., J. A. Davidson, A. H. McDaniel, R. E. Shetter, and J. G. Calvert, Infrared absorption cross-sections for N_2O_5, *Chem. Phys. Lett.*, *148*, 358–362, 1988.

Chance, K., et al., Simultaneous measurements of stratospheric HO_x, NO_x, and Cl_x: Comparison with a photochemical model, *J. Geophys. Res.*, *101*, 9031–9043, 1996.

Chang, A. Y., et al., A comparison of measurements from ATMOS

and instruments aboard the ER-2 aircraft: Halogenated gases, *Geophys. Res. Lett.*, *23*, 2393–2396, 1996a.

Chang, A. Y., et al., A comparison of measurements from ATMOS and instruments aboard the ER-2 aircraft: Tracers of atmospheric transport, *Geophys. Res. Lett.*, *23*, 2393–2396, 1996b.

Crutzen, P. J., The influence of nitrogen oxides on the atmospheric ozone content, *J. R. Meteorol. Soc.*, *96*, 320–325, 1970.

Dana, V., et al., Broadening parameters of NO_2 lines in the 3.4 μm spectral region, *J. Quant. Spectrosc. Radiat. Transfer*, *57*, 445–457, 1997.

DeMore, W. B., et al., Chemical kinetics and photochemical data for use in stratospheric modeling, *JPL Publ.*, *94-26*, 1994.

DeMore, W. B., et al., Chemical kinetics and photochemical data for use in stratospheric modeling, *JPL Publ.*, *97-4*, 1997.

Dessler, A. E., et al., Balloon-borne measurements of ClO, NO, and O_3 in a volcanic cloud: an analysis of heterogeneous chemistry between 20 and 30 km, *Geophys. Res. Lett.*, *20*, 2527–2530, 1993.

Fahey, D. W., et al., In situ measurements of total reactive nitrogen, total water, and aerosol in a polar stratospheric cloud in the Antarctic, *J. Geophys. Res.*, *94*, 11,299–11,315, 1989.

Fahey, D. W., et al., In situ measurements constraining the role of sulfate aerosols in mid-latitude ozone depletion, *Nature*, *363*, 509–514, 1993.

Gao, R. S., et al., Partitioning of the reactive nitrogen reservoir in the lower stratosphere of the southern hemisphere: Observations and modeling, *J. Geophys. Res.*, *102*, 3935–3949, 1997.

Gordley, L. L., et al., Validation of nitric oxide and nitrogen dioxide measurements made by Halogen Occultation Experiment for UARS platform, *J. Geophys. Res.*, *101*, 10,241–10,266, 1996.

Hanson, D. R., and A. R. Ravishankara, Heterogeneous chemistry of bromine species in sulfuric-acid under stratospheric conditions, *Geophys. Res. Lett.*, *22*, 385–388, 1995.

Hanson, D. R., A. R. Ravishankara, and E. R. Lovejoy, Reactions of $BrONO_2$ with H_2O on submicron sulfuric acid aerosol and the implications for the lowest stratosphere, *J. Geophys. Res.*, *101*, 9063–9069, 1996.

Iraci, L. T., and M. A. Tolbert, Heterogeneous interaction of formaldehyde with cold sulfuric acid: Implications for the upper troposphere and lower stratosphere, *J. Geophys. Res.*, *102*, 16,099–16,107, 1997.

Jaeglé, L., Stratospheric chlorine and nitrogen chemistry: Observations and modeling, Ph.D. dissertation, 159 pp., Calif. Inst. of Technol., Pasadena, 1995.

Jaeglé, L., et al., In situ measurements of NO_2/NO ratio for testing atmospheric photochemical models, *Geophys. Res. Lett.*, *21*, 2555–2558, 1994.

Johnston, H. S., Reduction in stratospheric ozone by nitrogen oxide catalysts from SST exhaust, *Science*, *173*, 517–522, 1971.

Jucks, K. W., et al., Ozone production and loss rate measurements in the middle stratosphere, *J. Geophys. Res.*, *101*, 28,785–28,792, 1996.

Kawa, S. R., et al., Interpretation of NO_x/NO_y observations from AASE-II using a model of chemistry along trajectories, *Geophys. Res. Lett.*, *20*, 2507–2510, 1993.

Keim, E. R., et al., Measurements of the NO_y-N_2O correlations in the lower stratosphere: Latitudinal and seasonal changes and model comparisons, *J. Geophys. Res.*, *102*, 13,193–13,212, 1997.

Kinnison, D. E., K. E. Grant, P. S. Connell, D. A. Rotman, and D. J. Wuebbles, The chemical and radiative effects of the Mount Pinatubo eruption, *J. Geophys. Res.*, *99*, 25,705–25,731, 1994.

Koike, M., et al., Impact of Pinatubo aerosols on the partitioning between NO_2 and HNO_3, *Geophys. Res. Lett.*, *21*, 597–600, 1994.

Kondo, Y., et al., Diurnal variation of nitric-oxide in the upper-stratosphere, *J. Geophys. Res.*, *95*, 22,513–22,522, 1990.

Kondo, Y., T. Sugita, R. J. Salawitch, M. Koike, and T. Deshler, The effect of Pinatubo aerosols on stratospheric NO, *J. Geophys. Res.*, *102*, 1205–1213, 1997.

Lary, D. J., et al., Carbon aerosols and atmospheric photochemistry, *J. Geophys. Res.*, *102*, 3671–3682, 1997.

Lippman, H. H., B. Jesser, and U. Schurath, The rate constants of $NO + O_3 \rightarrow NO_2 + O_2$ in the temperature range of 283–443 K, *Int. J. Chem. Kinet.*, *12*, 547–554, 1980.

Loewenstein, M., J. R. Podolske, K. R. Chan, and S. E. Strahan, Nitrous oxide as a dynamical tracer in the 1987 Airborne Antarctic Ozone Experiment, *J. Geophys. Res.*, *94*, 11,589–11,598, 1989.

May, R. D., and R. R. Friedl, Integrated band intensities of HO_2NO_2 at 220K, *J. Quant. Spectrosc. Radiat. Transfer*, *52*, 257–266, 1993.

McCormick, M. P., L. W. Thomason, and C. R. Trepte, Atmospheric effects of the Mt. Pinatubo eruption, *Nature*, *373*, 399–404, 1995.

McElroy, C. T., C. Midwinter, D. V. Barton, and R. B. Hall, A comparison of J-values from the composition and photodissociative flux measurement with model calculations, *Geophys. Res. Lett.*, *22*, 1365–1368, 1995.

McElroy, M. B., R. J. Salawitch, and K. Minschwaner, The changing stratosphere, *Planet. Space Sci.*, *40*, 373–401, 1992.

Michael, J. V., J. E. Allen Jr., and W. D. Brobst, Temperature dependence of the $NO + O_3$ reaction rate from 195 to 369 K, *J. Phys. Chem.*, *85*, 4109–4117, 1981.

Michelsen, H. A., R. J. Salawitch, P. O. Wennberg, and J. G. Anderson, Production of $O(^1D)$ from photolysis of O_3, *Geophys. Res. Lett.*, *21*, 2227–2230, 1994.

Michelsen, H. A., et al., Stratospheric chlorine partitioning: Constraints from shuttle-borne measurements of [HCl], [$ClNO_3$], and [ClO], *Geophys. Res. Lett.*, *23*, 2361–2364, 1996.

Morris, G. A., et al., Nitrogen partitioning in the middle stratosphere as observed by the Upper Atmosphere Research Satellite, *J. Geophys. Res.*, *102*, 8955–8965, 1997.

Newchurch, M. J., et al., Stratospheric NO and NO_2 abundances from ATMOS solar-occultation measurements, *Geophys. Res. Lett.*, *23*, 2373–2376, 1996.

Osterman, G. B., et al., Balloon-borne measurements of stratospheric radicals and their precursors: Implications for production and loss of ozone, *Geophys. Res. Lett.*, *24*, 1107–1110, 1997.

Pickett, H. M., and D. B. Peterson, Stratospheric OH measurements with a far-infrared limb observing spectrometer, *J. Geophys. Res.*, *98*, 20,507–20,515, 1993.

Pickett, H. M., and D. B. Peterson, Comparison of measured stratospheric OH with prediction, *J. Geophys. Res.*, *101*, 16,789–16,796, 1996.

Plumb, R. A., and M. K. W. Ko, Interrelationships between mixing ratios of long-lived stratospheric constituents, *J. Geophys. Res.*, *97*, 10,145–10,156, 1992.

Prather, M., Catastrophic loss of stratospheric ozone in dense volcanic clouds, *J. Geophys. Res.*, *97*, 10,187–10,191, 1992.

Ravishankara, A. R., and D. R. Hanson, Differences in the reactivity of type-1 polar stratospheric clouds depending on their phase, *J. Geophys. Res.*, *101*, 3885–3890, 1996.

Ray, G. W., and R. T. Watson, Kinetics of the reaction $NO + O_3 \rightarrow NO_2 + O_2$ from 212 to 422 K, *J. Phys. Chem.*, *85*, 1673–1676, 1981.

Renard, J.-B., et al., Vertical distribution of nighttime stratospheric NO_2 from balloon measurements: Comparison with models, *Geophys. Res. Lett.*, *24*, 73–76, 1997.

Rinsland, C. P., et al., ATMOS/ATLAS-2 measurements of stratospheric chlorine and reactive nitrogen partitioning inside and outside the November 1994 Antarctic vortex, *Geophys. Res. Lett.*, *23*, 2365–2368, 1996.

Rodriguez, J. M., M. K. W. Ko, and N. D. Sze, Role of heterogeneous conversion of N_2O_5 on sulphate aerosols in global ozone losses, *Nature*, *352*, 134–137, 1991.

Roscoe, H. K., and J. A. Pyle, Measurements of solar occultation: The error in a naive retrieval if the constituent's concentration changes, *J. Atmos. Chem.*, *5*, 323–341, 1987.

Roscoe, H. K., J. R. Drummond, and R. F. Jarnot, Infrared measurements of stratospheric composition, III, The daytime changes of NO and NO_2, *Proc. R. Soc. London A*, *375*, 507–528, 1981.

Russell, J. M., et al., Measurements of odd nitrogen compounds in the stratosphere by the ATMOS experiment on Spacelab 3, *J. Geophys. Res.*, *93*, 1718–1736, 1988.

Salawitch, R. J., et al., The distribution of hydrogen, nitrogen, and chlorine radicals in the lower stratosphere implications for changes in O_3 due to emission of NO_y from supersonic aircraft, *Geophys. Res. Lett.*, *21*, 2547–2550, 1994a.

Salawitch, R. J., et al., The diurnal variation of hydrogen, nitrogen, and chlorine radicals: Implications for the heterogeneous production of HNO_2, *Geophys. Res. Lett.*, *21*, 2551–2554, 1994b.

Sen, B., G. C. Toon, J.-F. Blavier, E. L. Fleming, and C. H. Jackman, Balloon-borne observations of midlatitude fluorine abundance, *J. Geophys. Res.*, *101*, 9045–9054, 1996.

Solomon, S., R. W. Portmann, R. R. Garcia, L. W. Thomason, and M. P. McCormick, The role of aerosol variations in anthropogenic ozone depletion at northern midlatitudes, *J. Geophys. Res.*, *101*, 6713–6727, 1996.

Stachnik, R. A., J. C. Hardy, J. A. Tarsala, and J. W. Waters, Submil-

limeterwave heterodyne measurements of stratospheric ClO, HCl, O_3, and HO_2: First results, *Geophys. Res. Lett.*, *19*, 1931–1934, 1992.

Stimpfle, R. M., et al., The response of ClO radical concentrations to variations in NO_2 radical concentrations in the lower stratosphere, *Geophys. Res. Lett.*, *21*, 2543–2546, 1994.

Tie, X. X., and G. Brasseur, The importance of heterogeneous bromine chemistry in the lower stratosphere, *Geophys. Res. Lett.*, *23*, 2505–2508, 1996.

Toon, G. C., The JPL MkIV interferometer, *Opt. Photonics News*, *2*, 19–21, 1991.

Webster, C. R., R. D. May, R. Toumi, and J. A. Pyle, Active nitrogen partitioning and the nighttime formation of N_2O_5 in the stratosphere: Simultaneous in situ measurements of NO, NO_2, HNO_3, O_3, and N_2O using the BLISS diode-laser spectrometer, *J. Geophys. Res.*, *95*, 13,851–13,866, 1990.

Webster, C. R., R. D. May, M. Allen, L. Jaeglé, and M. P. McCormick, Balloon profiles of stratospheric NO_2 and HNO_3 for testing the heterogeneous hydrolysis of N_2O_5 on sulfate aerosols, *Geophys. Res. Lett.*, *21*, 53–56, 1994.

Wennberg, P. O., et al., Removal of stratospheric O_3 by radicals in situ measurements of OH, HO_2, NO, NO_2, ClO, and BrO, *Science*, *266*, 398–404, 1994.

Yue, G. K., L. R. Poole, P.-H. Wang, and E. W. Chiou, Stratospheric aerosol acidity, density, and refractive index deduced from SAGE II and NMC temperature data, *J. Geophys. Res.*, *99*, 3727–3738, 1994.

J.-F. Blavier, J. J. Margitan, G. B. Osterman, R. J. Salawitch, B. Sen, and G. C. Toon, Jet Propulsion Laboratory, California Institute of Technology, M. S. 183-301, 4800 Oak Grove Drive, Pasadena, CA, 91109-8099. (e-mail: sen@mark4sun.jpl.nasa.gov)

G. K. Yue, NASA Langley Research Center, M. S. 475, Hampton, VA 23681.

(Received April 1, 1997; revised August 12, 1997;
accepted August 27, 1997.)